Development 137, 333-345 (2010) doi:10.1242/dev.035964

DiSUMO-like DSUL is required for nuclei positioning, cell specification and viability during female gametophyte maturation in maize

Kanok-orn Srilunchang, Nádia Graciele Krohn and Thomas Dresselhaus*

SUMMARY

Reversible post-translational modification of numerous proteins by small ubiquitin-related modifiers (SUMOs) represents a major regulatory process in various eukaryotic cellular and developmental processes. To study the role of sumoylation during female gametophyte (FG) development in maize, we identified *Zea mays* genes encoding SUMO (ZmSUMO1a and ZmSUMO1b) and a diSUMO-like protein called ZmDSUL that contains two head-to-tail SUMO-like domains. Whereas *ZmSUMO1a* and *ZmSUMO1b* are almost ubiquitously expressed, *ZmDSUL* transcripts were detected exclusively in the egg apparatus and zygote. *ZmDSUL* was selected for detailed studies. ZmDSUL is processed close to the C-terminus, generating a dimeric protein that is similar to animal FAT10 and ISG15, which contain two ubiquitin-like domains. Whereas GFP fused to the ZmDSUL N-terminus was located in the cytoplasm and predominately in the nucleoplasm of some transiently transformed maize suspension cells, C-terminal GFP fusions exclusively accumulated at the nuclear surface. GFP or ZmDSUL-GFP under control of the *ZmDSUL* promoter first displayed GFP signals in the micropylar-most position of the FG at stage 5/6, when migration of polar nuclei and cellularization occurs. Mature FGs displayed GFP signals exclusively in the egg cell, but the strongest signals were observed shortly after fertilization and disappeared during the first asymmetric zygotic division. RNAi silencing of *ZmDSUL* showed that it is required for FG viability. Moreover, nuclei segregation and positioning defects occurred at stage FG 5 after mitotic nuclear divisions were completed. In summary, we report a diSUMO-like protein that appears to be essential for nuclei segregation and positioning, the prerequisite for cell specification during FG maturation.

KEY WORDS: Sumoylation, Female gametophyte, Egg cell, Polarity, Aggresome, *Zea mays*

INTRODUCTION

Reversible post-translational modifications are widely used to dynamically regulate protein activity and degradation. Proteins can be modified by small chemical groups, sugars, lipids and even by covalent attachment of other polypeptides. Ubiquitin, a highly conserved polypeptide of 76 amino acids, is the best-known and most widely studied example of a polypeptide modifier (Herrmann et al., 2007). It has been shown that conjugation of polyubiquitin chains (polyubiquitylation) involving lysine residue K48 has a well-established role in marking proteins for degradation by the 26S proteasome multi-enzyme complex (Müller et al., 2001). K29 and K63 polyubiquitylation lead to endosome formation and modification of protein function. Monoubiquitylation and polyubiquitylation can also direct target proteins towards the endosome-lysosome pathway (Haglund and Stenmark, 2006).

Since the discovery of ubiquitin, several related small proteins displaying structural similarity to ubiquitin have been reported (Gill, 2004; Herrmann et al., 2007; Kirkin and Dikic, 2007). These small ubiquitin-like proteins (UBLs) include small ubiquitin-like modifiers (SUMOs), related to ubiquitin 1 (RUB1/NEDD8), autophagy defective 8 (APG8) and APG12, homologous to ubiquitin 1 (HUB1/UBL5), ubiquitin fold modifier 1 (UFM1), ubiquitin-related modifier 1 (URM1) and Fau ubiquitin-like protein 1 (FUB1). Moreover, two UBLs containing two head-to-tail ubiquitin-like domains have been reported: interferon-stimulated gene 15 (ISG15) and antigen F-adjacent transcript 10 [FAT10; also known as ubiquitin D (UBD)]. Human SUMO1-3 (corresponding to yeast SMT3C, B and A, respectively) have been studied most intensively (Kirkin and Dikic, 2007).

SUMOs, which were first described in 1996, constitute a highly conserved protein family found in all eukaryotes (Johnson, 2004). Although SUMO shares only ~18% sequence identity with ubiquitin, their protein structures are similar (Gill, 2004). SUMO and ubiquitin share the same overall mechanistic principles of substrate selection and attachment, including a flexible C-terminus, which is generally a glycine residue that forms an isopeptide linkage to a lysine side chain within the target protein (Schwartz and Hochstrasser, 2003). The most prominent difference between members of the SUMO family and other ubiquitin-related proteins (including ubiquitin) is a very flexible N-terminal extension and an extension of amino acids at the C-terminus in SUMO (Melchior, 2000). The C-terminus is processed by limited proteolysis to expose a C-terminal glycine residue for target linkage (Kerscher, 2007). Whereas yeast and invertebrates studied to date contain a single *SUMO* gene, vertebrates contain four genes (*SUMO1-4*) and plants even more. For example, eight *SUMO* genes are found in the *Arabidopsis thaliana* genome (Saracco et al., 2007). Human SUMO2 and SUMO3 are ~96% identical (and are referred to collectively as SUMO2/3), whereas they share only ~45% identity with SUMO1 (Zhang et al., 2008). Interestingly, whereas human SUMO1 is apparently incapable of self-conjugation, SUMO2/3 can lead to chain formation (Tatham et al., 2001; Ulrich, 2008).

Cell Biology and Plant Biochemistry, University of Regensburg, Universitätsstraße 31, 93053 Regensburg, Germany.

*Author for correspondence (thomas.dresselhaus@biologie.uni-regensburg.de)

Accepted 5 November 2009

The reversible attachment of SUMO to target proteins (sumoylation) proceeds in analogy with that of ubiquitin. In an initial ATP-dependent process, SUMO forms a thioester bond with the heterodimeric SUMO-activating enzyme (SAE) (Desterro et al., 1999). The activated SUMO moiety is subsequently passed to SUMO-conjugating enzyme (SCE), which acts in concert with E3 ligases to attach SUMO to its targets through an isopeptide bond. In contrast to ubiquitin, the SUMO system utilizes only a single E2 enzyme, UBC9 (ubiquitin-conjugating enzyme 9), and probably fewer E3 ligases (Anckar and Sistonen, 2007). Moreover, UBC9 can recognize the substrate itself and directly transfers activated SUMO by the formation of an isopeptide bond between the C-terminal carboxyl group of SUMO and the ε-amino group of lysine in substrate proteins (Welchman et al., 2005). Desumoylation is catalyzed by cysteine proteases called ubiquitin-like-protein-specific protease 1 and 2 (Ulp1 and Ulp2) in yeast and sentrin/SUMO-specific proteases (SENPs) in human. Whereas SENP1 and SENP2 are able to process all three sumoylating isoforms without distinction, SENP3 and SENP5 display a preference for SUMO2/3. Interestingly, all of these proteases exhibit distinct subcellular localizations that match the function of their substrates: SENP1 localizes to the nucleus, SENP3 and SENP5 to the nucleolus and SENP2 to the cytoplasm, nuclear pore or nuclear body (reviewed by Herrmann et al., 2007).

Compared with ubiquitin, SUMO has many fewer cellular substrates but, intriguingly, several of these targets have turned out to be important cellular and especially transcriptional regulators (Geiss-Friedlander and Melchior, 2007; Gill, 2004; Müller et al., 2001; Vertegaal et al., 2006). Recently, it has become clear that sumoylation is involved in surprisingly diverse biological pathways, such as genome integrity, chromosome packing and dynamics, transcriptional regulation, nucleocytoplasmic translocalization and various aspects of signal transduction, acting via modulation of protein-protein interactions as well as protein-DNA binding (Hay, 2005). Through biochemical and proteomic approaches, over 200 proteins have been identified as SUMO substrates (Vertegaal et al., 2006; Zhang et al., 2008), implicating sumoylation as a post-translational modification mechanism with a wide range of cellular and developmental functions, predominately associated with the nucleus (Seeler and Dejean, 2003). Genetic studies have identified roles for sumoylation in regulating chromosome condensation and segregation via sister chromatid cohesion, kinetochore function, as well as mitotic spindle elongation and progression through mitosis (Watts, 2007).

Proper functioning of these processes is a major prerequisite for cell specification and fate determination during the development of higher eukaryotes. In order to understand the underlying molecular mechanisms of cell polarity establishment and cell identity in flowering plants (angiosperms), we are studying the development of the haploid female gametophyte (FG), or embryo sac, as a model. After meiosis, development of the angiosperm embryo sac begins with a phase of free nuclear division to produce an eight-nucleus coecytium during a process termed megagametogenesis. During this process, embryo sac nuclei undergo a stereotypical number of mitotic divisions. Migration and asymmetric positioning of the nuclei is highly regular. The embryo sac then cellularizes and differentiates to produce four cell types: an egg cell, usually two synergids, a homodiploid central cell and, depending on the plant species, up to ~40 antipodals (Brukhin et al., 2005; Drews and Yadegari, 2002). Embryo sac development thus provides an ideal system with which to study fundamental cellular processes such as asymmetric nuclear positioning and migration, as well as position-dependent cell fate determination.

As sumoylation plays a prevalent role in functions associated with the mitotic nucleus, we searched maize and wheat egg cell EST data (Márton et al., 2005; Sprunck et al., 2005) for transcripts encoding SUMO and SUMO-related proteins for further functional studies during FG development. Here, we report the identification of ubiquitously expressed *SUMO* genes and of a gene encoding a diSUMO-like (DSUL) protein that displays a highly specific expression pattern during embryo sac development and early embryogenesis in maize. Unlike FAT10 and ISG15, which contain two UBL domains, DSUL contains two head-to-tail SUMO-like domains, constituting the first report of such a structure. We further analyzed the phylogeny, processing, subcellular localization and expression pattern of DSUL, as well as its role during FG development.

MATERIALS AND METHODS

EST sequencing and bioinformatic analyses

A total of 988 EST sequences derived from a cDNA library of maize egg cells (Dresselhaus et al., 1994) were clustered and analyzed for the presence of transcripts encoding SUMO/SMT3 proteins. ZmSUMO1a (GenBank accession FJ515939), ZmSUMO1b (GenBank accession FJ515940) and ZmDSUL (GenBank accession FJ515941) sequences were compared online and aligned by ClustalW (Thompson et al., 1994). Alignment data were used to generate a phylogram (see Fig. 2) with TreeView (version 1.6.6) (Page, 1996). Protein alignments were drawn by GeneDoc version 2.6.02 (Nicholas et al., 1997) using ClustalW alignment data. Prediction of three-dimensional (3D) protein structures was performed using HHpred (http://toolkit.tuebingen.mpg.de/hhpred) based on PDB 1Z2M structural data. Based on hits to known protein structures from HsISG15, the structure of ZmDSUL was modeled using Discovery Studio 1.7 (Accelrys).

Plant growth, isolation of cells from the female gametophyte and in vitro suspension culture

Maize (*Zea mays*) inbred lines A188 (Green and Phillips, 1975) and H99 (D'Halluin et al., 1992) and transgenic lines were grown under standard greenhouse conditions at 26°C with 16 hours light and a relative air humidity of ~60%. Cells of the maize embryo sac before fertilization were isolated according to Kranz et al. (Kranz et al., 1991) and after fertilization according to Cordts et al. (Cordts et al., 2001) with the exception that ears were kept on wet paper instead of MS medium. Tobacco (*Nicotiana benthamiana*) plants were grown at 22°C with 16 hours light and at 18°C in the dark with a relative air humidity of ~70%. Black Mexican Sweet (BMS) maize cells were cultivated in MS medium (Murashige and Skoog, 1962) containing 2 mg/l 2,4-dichlorophenoxyacetic acid (2,4D). Stock cultures on solid and suspension cultures in liquid MS medium were maintained in the dark at 26°C on a shaker at 60-70 rpm and subcultured into fresh medium every 3 weeks and 4 days, respectively.

DNA and RNA extraction, Southern blots and single-cell RT-PCR

Extraction of genomic DNA from plant tissues was performed as previously described (Pallotta et al., 2000). Total RNA was extracted from all samples using TRIzol (Invitrogen) according to the manufacturer's specifications. Before RT-PCR, 1 μg of total RNA was digested with DNaseI (DNaseI amp grade, Invitrogen) and used for first-strand cDNA synthesis using oligo(dT)$_{18}$ (MBI Fermentas) and reverse transcriptase (RevertAid M-MuLV Reverse Transcriptase, MBI Fermentas) following the manufacturer's protocol. The quality and amount of cDNAs generated were analyzed by PCR using the maize *GAPDH* (*glyceraldehyde 3-phosphate dehydrogenase*)-specific primers ZmGap1 (5′-AGGGTGGTGCCAA-GAAGGTTG-3′) and ZmGap2 (5′-GTAGCCCCACTCGTTGTCGTA-3′). For detection of transgenic plants, mRNA from plant leaves was isolated using Dynabead oligo(dT)$_{25}$ (Invitrogen) following the manufacturer's guidelines. cDNA was generated as described above.

For Southern blot analysis, genomic DNA was digested with *Bsp*TI and *Not*I. This enzyme combination cuts out the full-length *ZmDSUL* cDNA from the pZmDSUL-RNAi vector described below. Restricted DNA was separated in 1% agarose gels and transferred with 20×SSC onto Hybond-

XL membranes (GE Healthcare). DNA was cross-linked to membranes with 300 mJ radiation in a UV Stratalinker 1800 (Stratagene). Hybridization, washing and exposure were performed according to the procedure described for DNA gel blots by the manufacturer (Roche).

Single-cell (SC) RT-PCR analysis was performed as described (Cordts et al., 2001) with minor modifications. SC reverse transcription was performed using primers ZmDSULRev (5′-GCTGCCATCAATGATG-GAGCAG-3′), ZmSUMO1aRev (5′-GTCCCTCAGCAATGGCACAAG-3′) or ZmSUMO1bRev (5′-CAAGGAGCCAGAGCATCACAAG-3′) in addition to ZmGap2 (5′-GTAGCCCCACTCGTTGTCGTA-3′) for cDNA synthesis. After reverse transcription, each reaction was split in two and 38 PCR cycles were conducted with each reaction using: *ZmDSUL*-specific primers, ZmDSULFor (5′-CGATCAGGCTTCAGGCATGGC-3′) and ZmDSULRev; *ZmSUMO1a*-specific primers, ZmSUMO1aFor (5′-CGC-CCGGAAACTGACCTCTACC-3′) and ZmSUMO1aRev; *ZmSUMO1b*-specific primers, ZmSUMO1bfor (5′-ATCGATCGCCGGAAAAC-TAACC-3′) and ZmSUMO1bRev; and *GAPDH*-specific primers, ZmGap1 (5′-AGGGTGGTGCCAAGAAGGTTG-3′) and ZmGap2. Twenty-five microliters of the *ZmDSUL*, *ZmSUMO1a* and *ZmSUMO1b* and 15 µl of the *GAPDH* PCR products were separated in 1% agarose gels. The amplified *ZmDSUL* transcript was 753 bp, *ZmSUMO1a* 440 bp, *ZmSUMO1b* 415 bp, and *GAPDH* 622 bp. Maize *SUMO* and *DSUL* genes do not contain introns so *GAPDH*-derived genomic amplificates (~1.2-1.3 kb) were used to monitor for genomic DNA contamination.

Generation of constructs

pZmDSUL-RNAi construct (*Ubi*p::*ZmDSUL-AS*::*iF2intron*::*ZmDSUL*::*OCSt*)

ZmDSUL cDNA was PCR amplified from vector pUbi-IF2-15 (DNA Cloning Service, Hamburg) using primers F15Eco (5′-CGCGGAATTC-ACGATCAGGCTTCA-3′) and R15Bam (5′-CAGTGGATCCGGTTC-TCAATCGATGT-3′) and cloned in antisense orientation into the *Bam*HI and *Eco*RI sites (underlined) of the vector pUbi-ZmDSUL (DNA Cloning Service, Hamburg). In a second cloning step, *ZmDSUL* cDNA was PCR amplified using primers F15Bsr (5′-GCGGCCTGTACACGATCAGGC-TTCA-3′) and R15Bss (5′-CAGTGCGCGCGGTTCTCAATCGATGT-3′) from vector pUbi-IF2-15, and cloned in sense orientation into the *Bsr*GI and *Bss*HII sites (underlined) of the vector pUbi-ZmDSUL, generating the pZmDSUL-RNAi construct.

pZmDSUL:ZmDSUL-GFP (*ZmDSUL*p::*ZmDSUL-GFP*::*NOSt*) and pZmDSUL:GFP (*ZmDSUL*p::*GFP*::*NOSt*) vectors

For the first construct, the open reading frame (ORF) of *ZmDSUL* together with 1566 bp upstream of the ORF were PCR amplified from genomic DNA using primers 15Fgen (5′-CTCTGCGGCCGCTTTGCTCACAG-3′) and 15Rgen (5′-CCGGATCCAATAAAAATTATTAGCTGCC-3′), which contain *Not*I and *Bam*HI sites (underlined), respectively. The fragment was cloned between the *Not*I and *Bam*HI sites of the vector pLNU-GFP-Neu (DNA Cloning Service, Hamburg) to generate the pZmDSUL:ZmDSUL-GFP construct. For the shorter promoter construct, a PCR fragment was generated using primers pZm15_fw-SpeI (5′-GCATACTAGT-GCTTTGCTCACAGGTGATTCAG-3′) and pZm15_rev-EcoRI (5′-CGATGAATTCGCCTGAAGCCTGATCGTCCTTC-3′). The PCR fragment was inserted in front of the *Nos* terminator in the plasmid pNos-AM (DNA Cloning Service, Hamburg) using *Spe*I and *Eco*RI. In order to generate a short version of the promoter, the resulting plasmid was cut with *Eco*RV and *Stu*I and religated, resulting in a shortened promoter comprising the 511 bp upstream of the start codon. The GFP reporter cDNA was inserted between the promoter and terminator to produce the reporter construct.

pN-DSUL-GFP (*35S*p:*GFP*::*ZmDSUL*::*35S*t) and pC-DSUL-GFP (*35S*p::*ZmDSUL*::*GFP*::*35St*) constructs

The ORF of *ZmDSUL* DNA was PCR amplified from the plasmid pZmDSUL-ZmDSUL-GFP (see above) with modified primers ZmDSULgateFor (5′-CACCATGGCGTCCCCTGGCCGG-3′) and ZmDSULgateRev (5′-GGATCCATAAAAATTATTAG-3′) generating CACC and *Bam*HI restriction sites (underlined), respectively. PCR products were cloned using the pENTR Directional TOPO Cloning Kit (Invitrogen). Entry clones were generated using the Gateway System (Gateway LR Clonase II Enzyme Mix, Invitrogen) and the destination vectors pB7FWG2.0 for C-terminal GFP fusion to ZmDSUL and pB7WGF2.0 for N-terminal GFP fusion to ZmDSUL (Karimi et al., 2002). Plasmids were fully sequenced. Plasmids (generally 0.1 µg) were used for transformation of *E. coli* or cells of *Agrobacterium tumefaciens* strain GV3101 (Holsters et al., 1980) according to standard procedures.

Biolistic transformation and regeneration of transgenic maize plants

Biolistic transformation of BMS suspension cells was performed as follows. Cells were grown at 26°C in a dark chamber with shaking at 60-70 rpm. Before transformation, cells were sterile filtered through a 500 µm metal net and then passed through a 100 µm pore-size nylon mesh to spread a uniform cell layer on solid MS medium. Before biolistic transformation, cells were incubated at 26°C for 1-2 hours. After transformation, plates were incubated overnight in the dark at 26°C. Cells were transferred to fresh liquid medium and cultivated in the dark in a shaker (60-70 rpm) for at least 4 hours before microscopic observations. Photos were taken immediately after transfer onto glass slides of 100 µl of medium containing individual cells or cell clusters showing GFP fluorescence.

Transformation of immature maize embryos using biolistic particle bombardment was performed as follows. Immature hybrid embryos of the maize inbred lines A188 and H99 were isolated 11-13 days after pollination (DAP). The constructs pZmDSUL-RNAi, pZmDSUL-GFP and pZmDSUL-ZmDSUL-GFP were each co-transformed with the vector *35S*p:*PAT* carrying the selectable marker PAT for glufosinate ammonium resistance (Becker et al., 1994). Particle bombardment, tissue culture and selection of transgenic maize plants were performed using standard procedures (Brettschneider et al., 1997).

Recombinant protein expression in *Nicotiana benthamiana*

To express recombinant ZmDSUL fusion proteins in *Nicotiana benthamiana*, *Agrobacterium tumefaciens* strain GV3101 was grown at 28°C in LB medium with 40 µg/ml gentamycin and 50 µg/ml spectomycin to the stationary phase. Bacteria were sedimented by centrifugation at 3500 ***g*** for 15 minutes at room temperature and resuspended in infiltration buffer (10 mM $MgCl_2$, 10 mM MES-KOH pH 5.7, 100 µM acetosyringone). Cells were left in this medium for 2 hours and then infiltrated into the abaxial air spaces of 2- to 4-week old *Nicotiana benthamiana* plants. *Agrobacterium* cultures carrying ZmDSUL-fusion protein (N- and C-terminal GFP versions) were mixed 1:1 with an *Agrobacterium* culture containing a p19 construct to suppress post-transcriptional gene silencing (PTGS) of the host silencing response to increase transient gene expression (Voinnet et al., 2000; Voinnet et al., 2003). The cultures were brought to an optical density (OD_{600}) of a maximum of 1.0 to avoid toxicity.

For total protein extraction, 1 g of *N. benthamiana* leaves was collected after 2 days infiltration and ground to a powder in a Retsch MM200 homogenizer for 2 minutes at 30 Hz. Protein extraction buffer [300-500 µl of 20 mM Tris-Cl pH 7.5, 150 mM NaCl, 1 mM EDTA, 10 mM DTT and protease inhibitor cocktail (one tablet per 10 ml of extraction buffer)] was added to the ground sample. Samples were centrifuged at 48,000 ***g*** for 1 hour at 4°C. Protein concentrations were determined by a standard Bradford assay (Bio-Rad). Thirty micrograms of the supernatant was then loaded onto a 12% SDS-PAGE gel or stored at –20°C for later analyses. Proteins were separated and transferred onto PVDF membranes (Millipore) by wet electroblotting. For detection of GFP, a mouse IgG κ monoclonal GFP antibody (Roche) and an anti-mouse IgG-POD antibody conjugated to peroxidase (Roche) were used at 1:5000 dilution. Signals were detected using the ECL Detection Kit (GE Healthcare).

Histological studies, GUS staining and GFP imaging

For phenotype analysis of wild-type and *ZmDSUL*-RNAi embryo sacs, immature and mature cobs were harvested from greenhouse-grown maize plants. Whole cobs were treated according to a fixing/clearing method using Kasten's fluorescent periodic acid-Schiff's reagent as described (Vollbrecht and Hake, 1995). The phases for hydration and dehydration of ears were prolonged from 20 to 30 minutes in each step and ears were dissected after they were cleared with methyl salicylate (Young et al., 1979). Samples were

mounted in methyl salicylate on glass slides under a coverslip and analyzed by confocal laser-scanning microscopy (CLSM) with a LSM 510-META microscope (Zeiss) with 488 nm excitation and an LP 505 filter.

GUS staining of maize ovaries at various stages of FG development was performed as follows. The various stages were dissected and incubated in GUS staining buffer as previously described (Bantin et al., 2001) with the exception that the staining solution was prepared in water. After 1-2 hours incubation at 37°C, dissected ovules were washed in 100 mM sodium phosphate buffer (pH 7.0) and placed on a glass slide with a drop of Hoyer's clearing solution for 15-20 minutes before microscopy. GFP fluorescence from BMS suspension cells and maize embryo sacs was monitored by CLSM with 488 nm excitation and a BP 505-550 filter for selective GFP visualization. Image capture and processing were performed using an AxioCam HRc camera, Zeiss LSM 510 META software and Zeiss LSM image browser version 3.5.0.359.

RESULTS

DSUL encodes a diSUMO-like protein localized to nucleoplasm and cytoplasm

Our previous studies and those of other labs have indicated that post-translational protein modification by ubiquitylation and sumoylation might play a major role in gametophyte development in plants (e.g. Sprunck et al., 2005; Borges et al., 2008; Kim et al., 2008; Liu et al., 2008). To study the role of SUMO during female gametophyte (FG) development, we searched for transcripts encoding SUMO in an EST collection from maize egg cells (Dresselhaus et al., 1994; Márton et al., 2005). Among the 30 largest EST clusters, we identified three genes encoding proteins with homology to SUMO (see Table S1 in the supplementary material). A more detailed analysis (Fig. 1A and Fig. 2) that compares these proteins with highly conserved ubiquitin and SUMOs from human (HsUbi, 76 amino acids; and HsSUMO1-4, 95-103 amino acids) as well as *Arabidopsis* (AtSUM1-6, 100-117 amino acids) revealed two highly similar proteins, named *Zea mays* SUMO1a/b (ZmSUMO1a and ZmSUMO1b, with precursor lengths of 99 and 109 amino acids, respectively), that were homologous to AtSUM1 and 2 (Fig. 2).

Interestingly, the third protein contained two head-to-tail SUMO-like domains and was named *Zea mays* diSUMO-like (ZmDSUL). For alignments and phylogenetic investigations, the ZmDSUL sequence, which consists of 250 amino acids, was split into two domains [ZmDSUL-N (126 amino acids) and ZmDSUL-C (124 amino acids)] after a putative di-glycine (GG) cleavage site typically found at the C-terminus of all SUMO proteins (the GG motif for sumoylation is boxed in red in Fig. 1A). Until now, no dimeric SUMO-like protein has been described. However, FAT10 and ISG15 (each 165 amino acids) contain two ubiquitin-like domains. As shown in Table S1 in the supplementary material, the sequence homology of both domains in FAT10 and ISG15 is higher when compared with ubiquitin (27/34% and 28/36%, respectively) than with SUMO (15/11% and 12/18%, respectively), whereas ZmDSUL shows higher sequence homology with SUMO (25/22%) than with ubiquitin (17/15%). Thus, ZmDSUL represents the first dimeric SUMO-like protein reported. Another transcript for a diSUMO-like

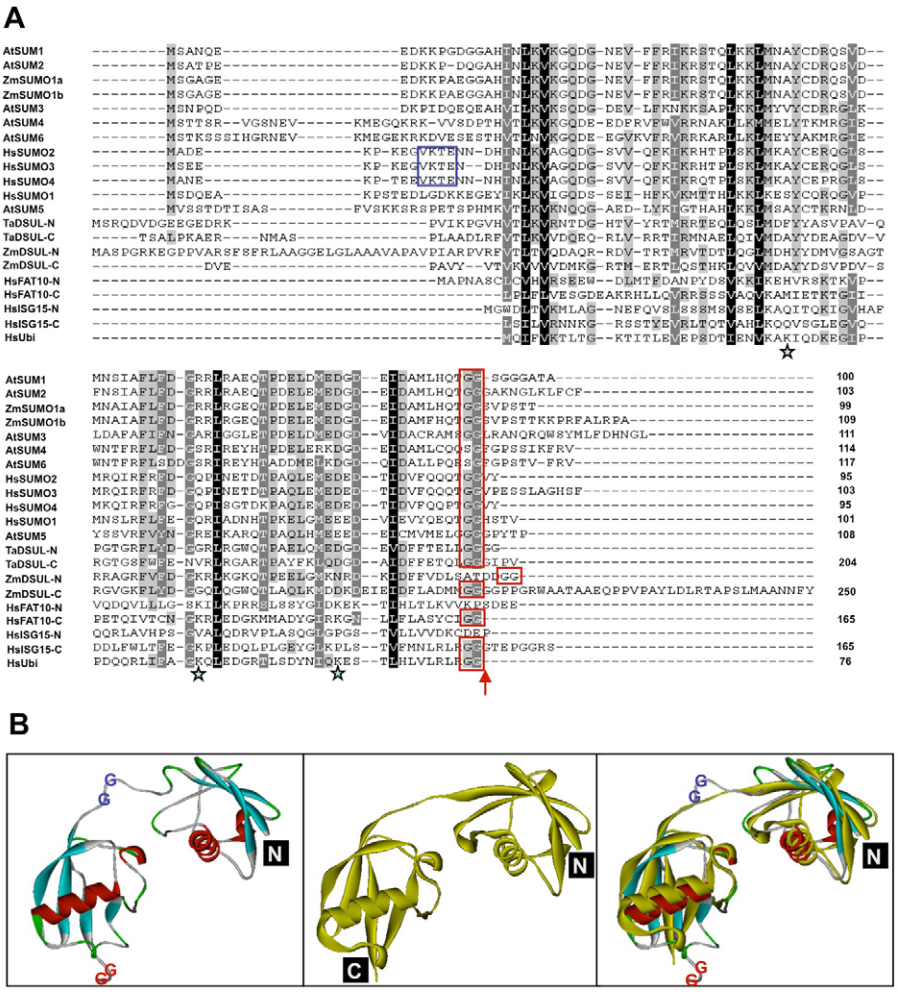

Fig. 1. Primary structure alignment of ubiquitin, diubiquitin-like, FAT10, ISG15, SUMO and DSUL proteins, and predicted 3D structure of ZmDSUL. (**A**) Protein sequences encoded by human (Hs), *Arabidopsis* (At), wheat (Ta) and maize (Zm) *Ubi* (*ubiquitin*), *SUMO* and *DSUL* genes were aligned using ClustalW and processed with GeneDoc. See Fig. 2 for protein accession numbers. Letters in black blocks indicate identical amino acid residues or conserved substitutions; amino acid residues with more than 80% conservation are highlighted in dark gray; and those with more than 60% conservation are highlighted in light gray. The dimeric SUMO-like (DSUL) proteins from maize and wheat as well as dimeric human ubiquitin-like FAT10 and ISG15 were split into an N-terminal and a C-terminal domain for alignment. Stars label Lys29, Lys48 and Lys63 in HsUbi, which serve as common sites for ubiquitin polymerization. The predicted cleavage sites (arrow) exposing C-terminal glycine-glycine (GG in red boxes) residues to generate mature SUMO and DSUL proteins are indicated and the length of precursor proteins is given. The N-terminal polysumoylation motif of HsSUMO2/3 and HsSUMO4 is boxed in blue. (**B**) Predicted 3D structure of ZmDSUL (left) based on the NMR structure of HsISG15 (middle; PDB IZ2M). N- and C-termini of proteins are indicated. ZmDSUL (left) forms two globular domains that are connected by a linker containing a putative SUMO cleavage site (blue GGs). Each domain consists of a β-sheet (light blue) and two α-helices (red). Loops/turns are indicated in green. GGs at the C-terminus are in red. An overlay of ZmDSUL and HsISG15 3D projections is shown (right).

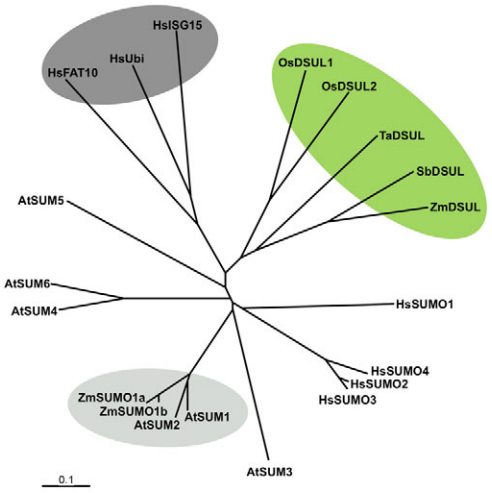

Fig. 2. Phylogenetic relationship of selected members of the ubiquitin (Ubi), diubiquitin-like (FAT10 and ISG15), SUMO and DSUL protein families. Protein sequences were aligned by ClustalW and the unrooted tree was drawn by TreeView. Branch lengths are proportional to phylogenetic distances and the scale bar represents 10% substitutions per site. Protein accession numbers at GenBank are as follows: *Zea mays* ZmSUMO1a (FJ515939), ZmSUMO1b (FJ515940), ZmDSUL (FJ515941); *Sorghum bicolor* SbDSUL (EER97428); *Triticum aestivum* TaDSUL (FJ515942); *Oryza sativa* OsDSUL1 (NP_001060074), OsDSUL2 (EAZ04433); *Arabidopsis thaliana* AtSUM1-6 (NP_194414, NP_200327, NP_200328, NP_199682, NP_565752 and NP_199681); and *Homo sapiens* HsSUMO1-4 (AAC50996, AAH71645, NP_008867 and NP_001002255), HsFAT10 (NP_006389), HsISG15 (NP_005092) and HsUbi (P62988). Genes encoding DSUL proteins have only been detected in Poaceae genomes and form their own clade (green). Maize SUMO proteins (ZmSUMO1a and ZmSUMO1b) form a highly homologous clade with *Arabidopsis* SUM1 and SUM2 proteins (light gray). HsFAT10 and HsISG15 are most closely related to ubiquitin (HsUbi as an example, dark gray).

protein consisting of 204 amino acids was identified in a wheat egg cell EST collection [named *Triticum aestivum* diSUMO-like (TaDSUL); Fig. 1A] (Sprunck et al., 2005).

Various plant genomes were then analyzed for the presence of DSUL-encoding genes. *Sorghum bicolour* contains a gene (*SbDSUL*) most similar to maize *DSUL*, and two less related *DSUL* genes were identified in the rice genome (Fig. 2). Dicotyledonous plant species, including *Arabidopsis thaliana*, poplar and vine grape, as well as the moss *Physcomitrella patens*, do not contain *DSUL* genes, indicating that they are Gramineae- or monocot-specific. Phylogenetic analyses showed that DSUL proteins form their own clade, whereas dimeric FAT10 and ISG15 form a clade with ubiquitin (Fig. 2). ZmSUMO1a and ZmSUMO1b cluster into the same group with AtSUM1 and AtSUM2.

The common sites for ubiquitin polymerization at Lys29 and Lys63 are missing in SUMO and DSUL sequences, indicating that polymerization does not occur. The conserved Lys48 residue found in ZmDSUL and SbDSUL is not present in wheat and rice DSUL. This indicates that this site might not be involved in polymerization, although biochemical proof is missing. With the exception of that from *Oryza sativa* (OsDSUL2), DSUL proteins contain two conserved predicted di-glycine (GG) processing sites, one in the middle and the other at the C-terminus. SUMO-specific proteases cleave after the GG site to expose these residues for activation and sumoylation (Herrmann et al., 2007). The absence of this motif in OsDSUL2 might indicate that it represents a pseudogene and that OsDSUL1 is the active rice protein. Three-dimensional structure modeling of ZmDSUL (Fig. 1B, left) based on the X-ray crystal structure of HsISG15 [1Z2M (Narasimhan et al., 2005); Fig. 1B, middle] not only showed that the structure of ZmDSUL is highly conserved and strongly overlaps with that of HsISG16 (Fig. 1B, right), but also that it consists of two globular domains linked by a long stretch containing the predicted GG processing site in the middle of the protein, as well as an exposed second GG site at the very C-terminus. In order to determine whether ZmDSUL is processed at either or both predicted cleavage sites, we fused GFP N- or C-terminally to ZmDSUL and transiently expressed the fusion proteins in tobacco (*Nicotiana benthamiana*) leaves. Two days after infection, crude protein extracts were separated by SDS-PAGE and analyzed by immunoblotting using an anti-GFP antibody (Fig. 3A). Lack of processing should generate 54 kDa bands. Processing behind the central GG site between both SUMO-like domains should give a 42 kDa band, and cleavage after the C-terminal GG site should generate a 52 kDa band for the N-terminal and a 32 kDa band for the C-terminal GFP fusions. A 31 kDa ER-GFP (GFP fused with the endoplasmic reticulum luminal target sequence KDEL) was used as a positive control. The N-terminal fusion showed a 52 kDa band and the C-terminal fusion a weak band at 32 kDa (Fig. 3A). Additionally, 34 kDa bands and a 31 kDa band for the N-terminal fusion were visible, probably derived from degradation products. A 42 kDa band was never detected. We conclude that ZmDSUL is only processed at the C-terminus and not in the middle of the protein, thus generating a naturally occurring diSUMO-like protein with an exposed di-glycine at the very C-terminus. The GFP degradation products that were always observed with both chimeric proteins suggest that maize DSUL might not possess a very long half-life in tobacco leaves.

We used the same constructs to study the subcellular localization of ZmDSUL in maize Black Mexican Sweet (BMS) cell suspensions. As shown in Fig. 3B-E, GFP signals from the N-terminal fusion protein were evenly distributed in the cytoplasm and nucleoplasm, excluding the nucleolus. About one-third of the cells showed stronger accumulation inside the nucleus (Fig. 3B). Interestingly, when GFP was fused to the C-terminus of ZmDSUL, from where it is cut (Fig. 3A), fluorescence signals were exclusively detected polar at one cytoplasmic site of the nuclear surface, but not in the nucleoplasm nor in the remainder of the cytoplasm (Fig. 3F-I). Similar protein localization and aggregation have been described previously for animal cells that accumulate unfolded or misfolded proteins at the pericentriolar region in the immediate vicinity of the nucleus. This region has also been shown to contain many proteasome complexes and has been termed the aggresome in animal cells (Hatakeyama and Nakayama, 2003). Similar localization was not observed when GFP was fused to the N-terminus of ZmDSUL, nor in cells expressing very high amounts of free GFP. Free GFP always showed equal fluorescence in the cytoplasm and nucleus, excluding the nucleolus (Fig. 3J,K).

ZmDSUL is exclusively expressed in the micropylar region of the immature female gametophyte and is restricted to egg cell and zygote after cellularization

We first analyzed the expression pattern of *ZmSUMO1a*, *ZmSUMO1b* and *ZmDSUL* in various maize tissues and cells of the FG by RT-PCR. As shown in Fig. 4A, *ZmSUMO1b* was ubiquitously expressed in all tissues analyzed, whereas *ZmSUMO1a*

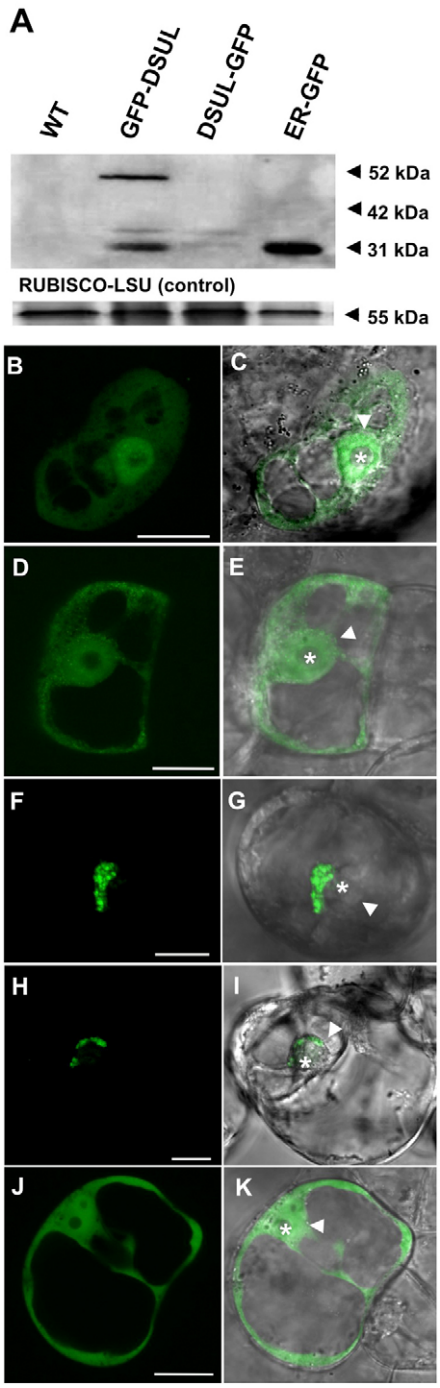

Fig. 3. Processing and subcellular localization of ZmDSUL. Processing of ZmDSUL was studied 2 days after infection of *Nicotiana benthamiana* leaves and subcellular localization in maize suspension cells after transient transformation. (**A**) Dimeric ZmDSUL is processed at the C-terminus, but is not cleaved to generate monomeric DSUL protein domains. Two days after infiltration (infection) with the constructs described below, tobacco leaf protein extracts were blotted and the length of GFP-fusion proteins detected with an anti-GFP antibody. The full-length fusion protein (52 kDa) was only detected when GFP was fused to the N-terminus (GFP-DSUL). GFP cleaved from the predicted C-terminal di-glycine motif generates a band at 32 kDa. A fusion protein containing a monomeric ZmDSUL domain with GFP either attached to the N- or C-terminus (42 kDa) was never detected. ER-GFP (31 kDa) was loaded as a positive control. WT, wild type. (**B-E**) BMS suspension cells bombarded with gold particles carrying a construct *p35S:GFP-ZmDSUL* encoding GFP fused to the N-terminus of ZmDSUL. (B,C) In some cells, GFP signals were predominantly visible in the nucleus (arrowhead), but not in the nucleolus (asterisk). Strong GFP-ZmDSUL fluorescence was also visible in the cytoplasm, whereas the majority of cells showed an even distribution between nucleus and cytoplasm (D,E). (**F-I**) BMS suspension cells bombarded with gold particles harboring a *p35S:ZmDSUL-GFP* construct. Signals were exclusively detected in the cytoplasm, polar at the nuclear surface (F,H). (**J**,**K**) BMS suspension cells were bombarded with gold particles carrying a *pUbi:GFP* construct as a control. GFP signals are visible at equal intensities in the nucleus and cytoplasm, excluding the nucleolus. Arrowheads, nuclei; asterisks, nucleoli. (B,D,F,H,J) UV microscopy images; (C,E,G,I,K) UV images merged with their respective bright-field microscopy images. Scale bars: 20 μm.

was particularly expressed in vegetative and male reproductive tissues. By contrast, expression of *ZmDSUL* could not be detected in any of the vegetative and reproductive tissues analyzed. A more detailed expression analysis of these genes in isolated cells of the FG before and after fertilization (Fig. 4B) indicated relatively low transcript levels of *ZmSUMO1a* and *ZmSUMO1b* in both egg cells and zygotes (24 hours after pollination). Transcripts derived from synergids were detected after Southern blotting (data not shown). By contrast, *ZmDSUL* was highly expressed in egg cells and even more strongly in zygotes, confirming the maize egg cell EST cluster data in which *ZmDSUL* was identified as one of the most abundant ESTs. Significant expression was also detected after 38 PCR cycles in synergids, whereas expression in central cells and sperm cells was not detectable even by Southern blotting. Owing to its specific expression pattern in the FG, we restricted further analyses to *ZmDSUL*.

In order to study the onset of *ZmDSUL* expression during FG development, we cloned the 511-bp region upstream of its ORF as the short version of the *ZmDSUL* promoter (*ZmDSULp*). This promoter region was then used to drive expression of GFP as a marker in transgenic maize ovaries. As shown in Fig. 5A, GFP signals were first detectable at stage FG 5/6, when cellularization and nuclei migration takes place (see Fig. 6 for stages of FG development). GFP signals were visible in the micropylar-most region, where they accumulated in two of the four nuclei. After cellularization, GFP signals were exclusively detected in the immature egg cell (Fig. 5B). Whereas signal intensity decreased slightly during FG and egg cell maturation (Fig. 5C), a ~5-fold increase in signal intensity was observed in the zygote after fertilization (Fig. 5D) and signals completely vanished after the first asymmetric cell division (Fig. 5E). Expression at later stages during embryo development or outside the FG was never observed.

To analyze the formation of the aggresome-like structures described above during FG development, we cloned the 1566-bp region upstream of the ZmDSUL-ORF as the long promoter version. This promoter region was then used to control the expression of GFP fused C-terminally to ZmDSUL. The GFP expression pattern (Fig. 5F-J) was almost identical to that of free GFP, with the exception that GFP signals were first observed at the most-micropylar spindle pole region, excluding the nuclei. At later stages, GFP signals were strongest in the nucleus of egg cell and zygote, indicating that GFP might have been cleaved from the C-terminus of ZmDSUL and was then able to penetrate the nucleus. Occasionally, slight background

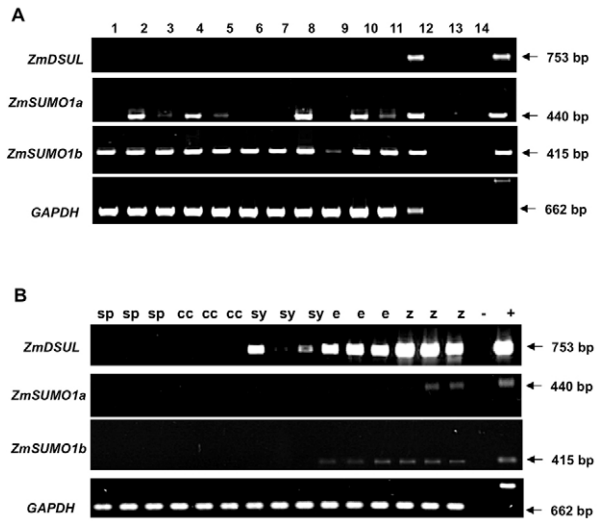

Fig. 4. Expression of *ZmDSUL*, *ZmSUMO1a* and *ZmSUMO1b* in various tissues and microdissected cells of the female gametophyte of maize before and after fertilization. (**A**) RT-PCR was performed on samples of various maize tissues using primers specific for *ZmDSUL*, *ZmSUMO1a*, *ZmSUMO1b* and *GAPDH*. Tissues are as follows: 1, embryo 10 days after pollination; 2, mature leaf; 3, root tips; 4, roots; 5, internodes; 6, nodes; 7, mature tassels; 8, mature pollen; 9, mature ovules; 10, mature anthers; 11, embryo 25 days after pollination; 12, egg cell; 13, water (negative control); 14, blank lane; 15, PCR from genomic DNA. (**B**) RT-PCR was performed on mRNA from individual cells of the female gametophyte. cc, central cell; e, egg cell; sp, sperm cells; sy, synergid; z, zygote, isolated 24 hours after pollination; –, blank lane; +, PCR from genomic DNA.

signals were visible at early stage FG7 in the antipodal region (Fig. 5B,G), but these were also visible in wild-type ovules of the same stages. In conclusion, 0.51 and 1.57 kb versions of the *ZmDSUL* promoter displayed the same activity during FG development, beginning at stage FG 5/6, restricted to the egg cell after cellularization and strongly induced again after fertilization, before being turned off before/during zygotic division. Moreover, aggresome formation was not observed when the endogenous promoter was used to study marker protein expression.

ZmDSUL is required for polar nuclei positioning, cell specification and viability during female gametophyte maturation

In order to investigate the role of ZmDSUL during FG and zygote/early embryo development, we first established a method to visualize megasporogenesis and megagametogenesis in maize. The size of the female inflorescence and silk length were measured and correlated with developmental stages as previously described (Huang and Sheridan, 1994). We adapted a method originally described by Young et al. (Young et al., 1979) with modifications (Vollbrecht and Hake, 1995). In order to understand whole FG structures, cleared ovules were sectioned and pieces containing FGs scanned by confocal laser-scanning microscopy (CLSM). Only sections with a cut face longitudinal to the mature FG could be fully scanned and taken into consideration when quantifying phenotypes.

Meiotic stages could be observed at a silk/female inflorescence length of 0-0.5 mm. Fig. 6A shows an enlarged subepidermal megaspore mother cell (archesporial cell). As differentiation and enlargement progressed, the nucleus became positioned towards the micropylar pole and the chromatin became condensed (pachytene stage in Fig. 6B). The nucleolus was still visible at the diplotene stage (Fig. 6C). Fig. 6D shows the ten homologous chromosome pairs aligned at the equatorial plate and the spindle apparatus is visible. Female meiosis finally results in a linear tetrad of four megaspores. The three megaspores orientated towards the micropyle degenerate (Fig. 6E,F), whereas the functional megaspore (stage FG 1) forms the mature FG after three mitotic nuclear divisions. At stage FG 1, a silk length of 0.5-1 mm was measured. After the first mitotic nuclear division (stage FG 2), the two nuclei were separated from each other by a large vacuole (Fig. 6G). The micropylar and chalazal poles were occupied by additional vacuoles. Further mitotic nuclear divisions occurred at both poles, first generating a four-nucleus (stage FG 3-4; silk length 1-4 mm, in Fig. 6H) and later an eight-nucleus (stage FG 5; silk length 4-5 mm, in Fig. 6I) immature FG. Between stages FG 5 and 6, one nucleus from each pole moved towards the center of the FG (Fig. 5I), approaching each other and remaining in direct contact. An eight-nucleus immature FG at late stage FG 6/early stage FG 7 (silk length 5-7 mm) is shown in Fig. 6J: polar nuclei have approached each other, egg and two synergid nuclei are visible in the micropylar region and antipodal cells are beginning to form at the chalazal pole. Finally, a fully mature and differentiated FG (at late stage FG 7; silk length 7 mm onwards) is shown in Fig. 6K: the egg cell and two synergids have been specified, polar nuclei of the central cell are positioned close to the egg cell, large vacuoles have formed inside the central cell and antipodals have divided to form a cluster of at least 20 cells.

An RNAi silencing approach using the maize Ubi1 promoter, which drives strong marker gene expression during megagametogenesis (see Fig. S1 in the supplementary material), was taken to downregulate *ZmDSUL* activity and to study its role during FG development, maturation and function. In contrast to wild-type plants (Fig. 7A), seed set was impaired in a number of independent transgenic *ZmDSUL*-RNAi lines. The RNAi lines #1 (accession #1513) and #2 (accession #1515) showed the most severe effect with ~35-44% undeveloped seeds in the T1 generation (Fig. 7B). Ears from these two independent heterozygous *ZmDSUL*-RNAi lines of the T2 generation (Table 1) were collected at maturity (silk length of ~5 cm onwards) and subjected to a cytological analysis using the fixing/clearing method described above. Maternal sporophytic tissues of all ovaries were fully developed to maturity and no morphological differences were detectable between wild-type and *ZmDSUL*-RNAi ovaries. Wild-type control plants contained ~96% fully differentiated FGs (Fig. 6K, Table 1). By contrast, heterozygous *ZmDSUL*-RNAi ovaries contained only ~67-74% differentiated FGs (Table 1).

A more detailed analysis revealed a variety of phenotypes, but meiotic and mitotic nuclear divisions seemed to have been completed because all FGs contained eight nuclei (Fig. 7C-J) or a degenerated FG at a later stage of maturation (Fig. 7K-N). Including stage FG 4, FGs from mutant ovules were indistinguishable from those of wild-type plants (Fig. 7C,D). However, at stage FG 5 a number of ovules contained eight nuclei in the center of the FG (Fig. 7E-H); these were positioned at opposite poles in wild-type ovules (Fig. 6I). Additionally, the large central vacuole was missing. Moreover, nuclei were not properly separated from each other, a prerequisite for cell specification occurring at this stage of FG maturation. We also observed a number of FGs that displayed a more polar distribution of four nuclei at a slightly later developmental stage (Fig. 7H-J), but also in these FGs polar localization was not completed and nuclei were

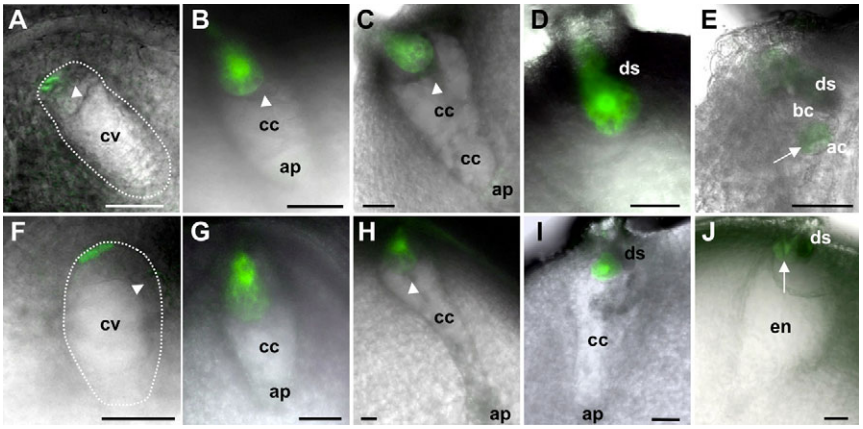

Fig. 5. *ZmDSUL* promoter activity is detectable in the micropylar region of the maize female gametophyte from stage FG 5 onwards and is restricted to egg cell and zygote after cellularization. Transgenic maize ovules expressing either GFP (A-E) or a C-terminal DSUL-GFP fusion protein (F-J) under the control of *ZmDSUL* promoters of 0.5 and 1.6 Kbp, respectively, were manually sectioned and scanned by confocal laser-scanning microscopy (CLSM). Note that free GFP is able to enter and thus label nuclei at various FG stages. (**A**) GFP signals are first detectable at stage FG 5/6 (whole FG encircled) and label the two uppermost of the four micropylar nuclei. A nucleus localized closer to the large central vacuole is not labeled (arrowhead) and signals in the chalazal region of the FG were never observed. (**B**,**C**) After cellularization and nuclei migration had been completed (early stage FG 7), strong GFP signals were restricted to the mature egg cell (B) and decreased slightly in intensity during FG maturation (late stage FG 7) (C). The arrowheads label the unfused polar nuclei of the central cell. (**D**,**E**) Strongest signals were detected after fertilization in the zygote (D) and signals completely vanished at the two-cell zygote (one-cell proembryo) stage (E). The arrow indicates the first asymmetric zygotic cell division plane. (**F**) Similar to GFP, DSUL-GFP signals were first detectable in the micropylar-most region of the FG at stage FG 5/6 (encircled), and were still excluded from nuclei. (**G**,**H**) Strongest signals before fertilization were detected in the egg cell at stage FG 7 (early) (G) and signal intensity slightly decreased during FG maturation (late stage FG 7) (H). (**I**,**J**) Similar to free GFP, signals obtained from DSUL-GFP were strongest in the zygote (I) and vanished after the first zygotic division (J, arrow). Note that GFP signals label the egg and zygote nucleus indicating that GFP was cleaved from the C-terminal end of DSUL. ac, apical cell; ap, antipodal cells; bc; basal cell; cc, central cell; cv, central vacuole; degenerated synergid cell; en, endosperm. Scale bars: 50 μm.

directly attached to each other and started to degenerate. Degeneration of the micropylar-most nuclei that specify the egg apparatus cells (two synergid cells and the egg cell) occurred first (Fig. 7H-J), and initiation of nuclear degeneration at the chalazal region was slightly delayed. When very mature ovaries at late stage FG 7 were analyzed, a relatively large number of ovaries showed disintegration of FG nuclei and cytoplasm and were collapsed or appeared empty (Fig. 7K-N). The frequency at which each phenotype occurred is shown in Table 1. The RNAi lines #1 and #2 were analyzed while silks from the ears had a maximum length of ~6 mm, corresponding to FG maturation stage FG7. Mutant ovaries displayed a developmental arrest at stage FG 5/6. Very mature mutant ovaries (RNAi line #2 with a silk length greater than 6 mm) analyzed at late stage FG 7 showed one-third collapsed or empty FGs.

We conclude that megagametogenesis is not affected by *ZmDSUL* downregulation until stage FG 5, which correlates with the onset of *ZmDSUL* promoter activity. All mitotic divisions were completed, but nuclei neither properly positioned at FG poles nor sufficiently separated from each other. In consequence, specification of the egg cell, synergid, central cell and antipodal cell could not take place and the FG instead disintegrated without affecting the maturation of surrounding maternal tissues.

DISCUSSION

Cell specification and viability of the female gametophyte

Although the maturation of the angiosperm FG is an attractive system with which to study fundamental cellular and developmental processes, such as asymmetric nuclear positioning and migration as well as position-dependent cell fate determination, until recently little progress had been made owing to the deep embedding of the embryo sac in the maternal tissues of the ovary. The establishment of powerful forward and reverse genetics methods combined with a toolkit of cellular markers has enabled these processes to be studied in the model plant *Arabidopsis* (Pagnussat et al., 2005; Jones-Rhoades et al., 2007; Berger et al., 2008) and has led researchers to the conclusion that the "angiosperm female gametophyte is no longer the forgotten generation" (Brukhin et al., 2005). However, until now only a few genes expressed in the FG have been studied at the functional level and we are just beginning to uncover the genes involved; for example, those involved in cell specification during embryo sac maturation (Gross-Hardt et al., 2007). In other plants, such as maize, which is especially suited to these studies owing to the large size of its embryo sac, until now only one report has described the molecular identity of a gene involved in position-based determination of FG cell identity. *IG1*, which encodes a LOB-domain protein, restricts nuclear division before cellularization (Huang and Sheridan, 1996; Evans, 2007). In contrast to *dsul* mutant phenotypes described in this report, the *ig1* mutant is viable in most genetic backgrounds. A large-scale genetic deficiency screen was conducted to characterize female gametogenesis in maize (Vollbrecht and Hake, 1995). Although this screen did not result in the identification of the genes involved, genetically separable female gametogenesis programs were identified and it was further demonstrated that embryo sac development requires post-meiotic gene expression. In conjunction with the *dsul* phenotypes, it is noteworthy that many of the mutant embryo sacs described had degenerated and degeneration often began at the micropylar pole, where *DSUL* is expressed. Moreover, some mutant embryo sacs defective in cellular patterning/cell specification contained nuclei of a different size and, occasionally, partly degenerated micronuclei, similar to findings in *dsul* mutant ovaries. The cytological analysis of partly sterile *indica/japonica* hybrids in rice indicated that sterility was mainly caused by FG development defects (Zeng et al., 2009). The phenotypes described partly overlap with those described for *dsul* mutant ovaries: the eight-nucleus stage was shown to be most severely affected by asynchronous nuclear migration and abnormal positioning of nuclei, as well as egg apparatus or complete FG degeneration. From our observations using young and very mature

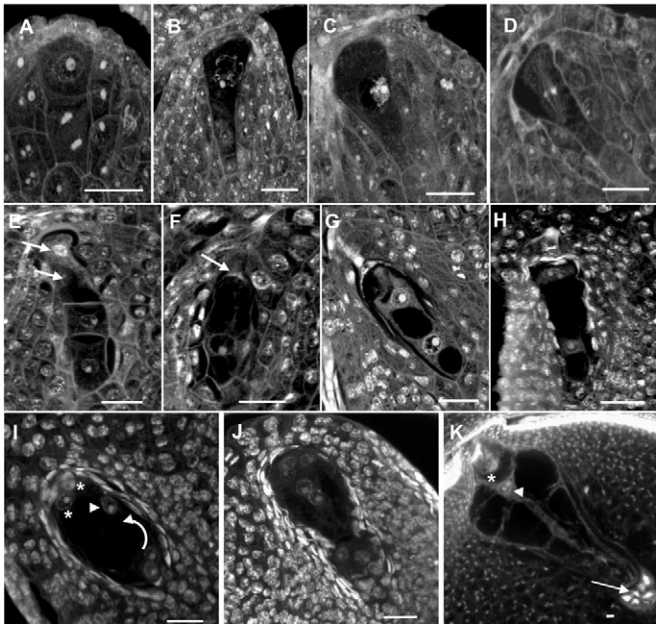

Fig. 6. Longitudinal CLSM sections of maize ovules to visualize nuclear division and migration during megasporogenesis and megagametogenesis. (**A**) Subepidermal megaspore mother cell (MMC) before the first meiotic division. (**B-D**) MMC at pachytene stage (B), at diplotene stage (C) and at metaphase I (D). (**E**) Quartet megaspore stage formed after meiosis. The two micropylar megaspores have started to degenerate (arrows). (**F**) The three micropylar megaspores are degenerated (arrow). The remaining large nucleus represents the functional megaspore (stage FG 1). (**G**) Two-nucleus female gametophyte (FG) stage (stage FG 2). Nuclei are separated by a large vacuole. (**H**) Four-nucleus FG (stage FG 3/4). (**I**) Eight-nucleus immature FG (stage FG 5/6) shortly before the polar nuclei approach each other. A nucleus from the micropylar region moves towards the upper center of the FG (arrowhead) to meet the second polar nucleus migrating at a longer distance (arrow) from the chalazal region of the immature FG. The egg nucleus and one synergid nucleus (asterisks) are visible in the micropylar region of the FG. (**J**) Eight-nucleus immature FG (late stage FG 6). Polar nuclei have approached each other, and the egg and two synergid nuclei are visible in the micropylar region and antipodal cells are beginning to form at the chalazal pole. (**K**) Mature FG (late stage FG 7). Egg cell (asterisk) and synergids are fully differentiated, polar nuclei (arrowhead) are positioned close to the egg cell and antipodals have divided to form a cluster of cells (arrow). Large vacuoles have formed in the cytoplasm of the central cell. Scale bars: 20 μm.

ovaries, we suggest that the latter phenotypes are likely to be a consequence of abnormal nuclear positioning, as well as of a failure of cell specification.

Does DSUL play a role in spindle elongation and asymmetry?

A detailed investigation of *dsul* mutant ovaries showed that mitotic nuclear division cycles were completed, but the eight nuclei of the immature FG were localized either centrally in the FG or not properly distributed towards the micropylar and chalazal poles. Moreover, nuclei were often not separated from each other, a prerequisite for cell specification. A similar phenotype has been described for *Arabidopsis* embryo sacs of double-heterozygous F1 mutants defective in both γ-*tubulin* genes. About 16% abnormal FGs were observed at the eight-nucleus stage, displaying an abnormal number, position and appearance of nuclei. Spindle and phragmoplast structures associated with cytokinesis were aberrant (Pastuglia et al., 2006). γ-tubulin, which is highly conserved, plays a major role in microtubule nucleation at microtubule-organizing centers (MTOCs) and thus in the establishment and organization of the mitotic spindle apparatus (Hendrickson et al., 2001).

SUMO has recently been reported to be a key regulator of mitotic spindle asymmetry in yeast (Leisner et al., 2008). It was shown that sumoylation of the spindle-orientation protein Kar9 regulates its asymmetric localization and thus positioning of both the spindle poles and the daughter nuclei. A number of reports showed an important role of sumoylation for chromosome segregation in yeast (reviewed by Watts, 2007). In mammalian cells, it has been shown that SUMO2/3 localize to centromeres and condensed chromosomes, whereas SUMO1 localizes to the mitotic spindle and spindle midzone (Zhang et al., 2008). In summary, the various reports indicate that sumoylation is essential for mitotic chromosome condensation, sister chromatid cohesion, kinetochore function, mitotic spindle elongation and asymmetry. Considering that *dsul* mutant embryo sacs contained eight nuclei, although not completely distributed to the poles and attached to each other, we suggest that DSUL might be involved in the

Table 1. Developmental defects of maize female gametophytes in *ZmDSUL*-RNAi lines

	n	Fully differentiated FGs (%)	Nuclei accumulate in FG center (%)	Unequal nuclei size (%)	Collapsed FG (%)	Empty FG (%)
						
Wild type*/†	63	96	0	0	4	0
RNAi #1*	97	74	7	5	14	0
RNAi #2*	129	74	4	8	14	0
RNAi #2†	110	67	0	2	16	15

Sporophytic tissues of the ovary were fully differentiated in wild-type and RNAi lines.
*Silk length 3-6 mm.
†Silk length >6 mm.
n, number of scanned embryo sacs.
FG, female gametophyte.

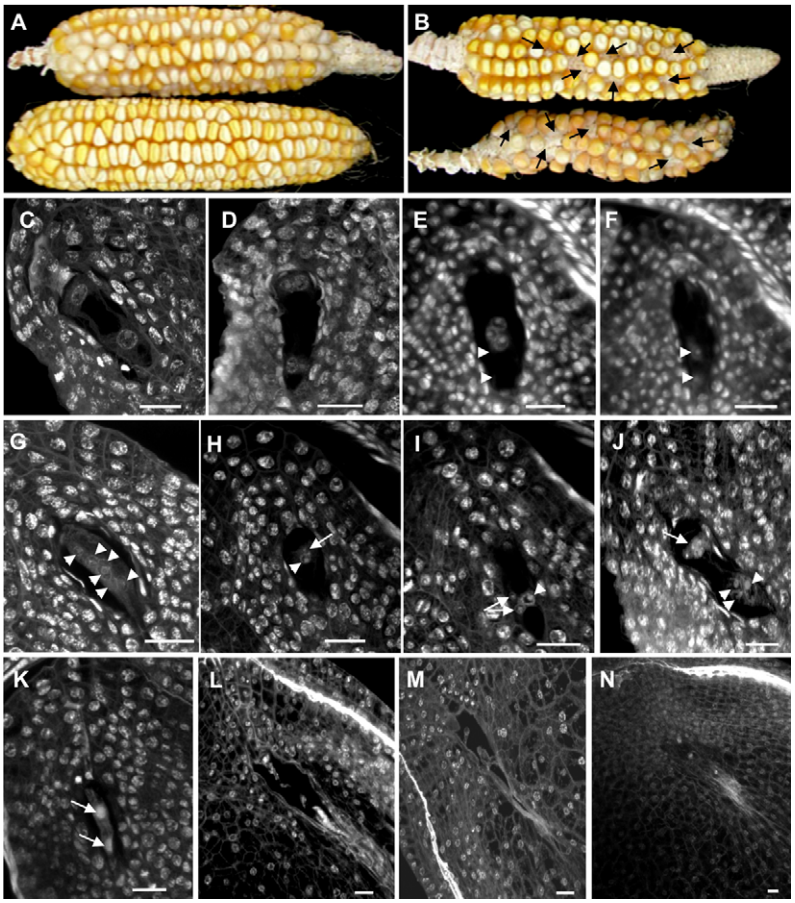

Fig. 7. Longitudinal CLSM sections of *ZmDSUL*-RNAi ovules reveal a lack of polar nuclei positioning and show nuclear degeneration at stage FG5/6 during megagametogenesis. (**A**) Ears from an A188 wild-type plant. (**B**) Ears from *ZmDSUL*-RNAi mutant plant line #1 (accession 1513, top) and #2 (accession 1515, bottom). Arrows indicate examples of ovaries that did not initiate seed development. (**C**,**D**) Ovules of heterozygous *ZmDSUL*-RNAi plants were analyzed after silk emergence. At this stage, the wild-type ovule contained fully differentiated and mature embryo sacs (stage late FG 7). FG development until stage FG 5/6 was identical to that of wild-type ovules as indicated by FGs from mutant plants at stages FG2 (C) and FG 4 (D). (**E-J**) Mutant ovules are arrested at stage FG 5/6. Nuclei are not properly positioned in the micropylar region of the FG, and the egg apparatus and antipodal regions are not specified. (E,F) Two focus planes of one mutant FG showing three (E) and two (F) of eight nuclei localized to the center of the FG (positions of the two nuclei shown in F are also indicated by arrowheads in E). (G) An example of six of eight nuclei (arrowheads) lined up from the micropylar to chalazal pole of the FG. Nuclei are not completely positioned at the poles. (H,I) Two focal planes of one mutant FG. (H) Three (arrow) of the four micropylar nuclei are already degenerated and not positioned in the micropylar-most region. One nucleus seems still intact (arrowhead). (I) Two of the four nuclei are already smaller and degenerating (arrows). The arrowhead marks an intact nucleus. (J) Similar phenotype as in H,I: a group of four nuclei at each pole are attached to each other; three of the four nuclei are not properly localized to the micropylar pole and have already degenerated (arrow), whereas nuclei at the chalazal pole seem still to be intact (arrowheads mark three of them in the focal plane shown). (**K**) Progression of nuclear degeneration at both poles (arrows). (**L**,**M**) Further progression of FG degeneration culminates in a tiny collapsed FG that lacks nuclei. (**N**) Overview of an ovule with a fully differentiated nuclear cone (top left) and inner integument containing an empty FG. Scale bars: 20 μm.

regulation of spindle elongation and asymmetry during megagametogenesis, and perhaps in asymmetric zygotic division, but that it is not, or is less, important for chromosome segregation itself.

ZmDSUL localization to the nucleoplasm and cytoplasm and aggresome formation

The unprocessed N-terminal ZmDSUL-GFP fusion protein displayed localization in both nucleoplasm and cytoplasm, with stronger accumulation in the nucleus, excluding the nucleolus, of some cells. A similar pattern has been described for the diubiquitin-like protein FAT10 (Kalveram et al., 2008). SUMO and sumoylation substrates are predominately nuclear, although a number of targets are also exclusively cytoplasmic (Herrmann et al., 2007; Seeler and Dejean, 2003; Vertegaal et al., 2006; Zhao, 2007). The subcellular localization pattern of GFP-ZmDSUL suggests that it might also be involved in modifying target proteins in both the cytoplasm and nucleoplasm. A very interesting subcellular localization pattern was observed when GFP was C-terminally fused to ZmDSUL and overexpressed in maize suspension cells. Localization of the fusion protein was exclusively perinuclear, at one site on the nuclear surface. Such an accumulation pattern has been reported previously for cytosolic GFP-fusion proteins that are either overexpressed, misfolded, inappropriately assembled, aberrantly modified or induced by environmental stress, and has thus been termed aggresome formation (Johnston et al., 1998; García-Mata et al., 1999; Kawaguchi et al., 2003). The aggresome comprises a huge proteasome complex located in immediate proximity to the

centrosome in animal cells. The cytoplasmic protein histone deacetylase 6 (HDAC6), which mediates the transport of polyubiquitylated cargo to the aggresome (Hubbert et al., 2002; Kawaguchi et al., 2003) was recently found to interact with FAT10 in animal cells. Endogenous and ectopically expressed FAT10, as well as FAT10-GFP, localized to the aggresome under proteasome-inhibiting conditions in a microtubule-dependent manner (Hipp et al., 2005; Kalveram et al., 2008). However, in contrast to our observations, N- and C-terminal fusions of GFP to FAT10 both displayed aggresome localization only under proteasome-inhibiting conditions, suggesting that ZmDSUL might possess functions additional to labeling proteins for degradation. Moreover, we did not observe aggresome formation in the FG using the *ZmDSUL* promoter, providing further evidence that the observed phenotype is solely correlated to overexpression of a cytosolic GFP-fusion protein, similar to observations made in animal cells (Johnston et al., 1998; García-Mata et al., 1999; Kawaguchi et al., 2003).

ZmDSUL structure and maturation

Based on the data presented here, we conclude that both ZmSUMO1a/b and ZmDSUL pre-proteins are C-terminally truncated to expose a di-glycine (GG) motif for sumoylation and dsulylation by DSUL, respectively. In contrast to the diubiquitin-like proteins FAT10 and ISG15, diSUMO-like DSUL from grasses contains the conserved GG motif also centrally and exposed between both SUMO-like domains. Biochemical studies in tobacco have revealed that DSUL is not cleaved at this position. Therefore, we conclude that DSUL represents a third member of the family of dimeric ubiquitin-related proteins. Another open question is related to the occurrence of polydsulylation by DSUL: whereas SUMO1 generally leads to monomodification, SUMO2/3 can lead to chain formation via the N-terminally located and conserved sumoylation motif ψKxE/D (where ψ is a large hydrophobic residue such as Val, Leu, Ile, Phe or Met and x is any amino acid) (Tatham et al., 2001; Matic et al., 2008). Whereas ZmDSUL and SbDSUL contain this motif only once in the middle of the C-terminal, and not N-terminal, SUMO-like domain, TaDSUL and OsDSUL1 do not contain this motif, indicating that polydsulylation by DSUL is unlikely to occur.

Although ZmDSUL is only ~13% homologous to HsISG at the amino acid level, we were able to predict a 3D model based on the available X-ray diffraction data for ISG15 (Narasimhan et al., 2005), conserved core amino acid positions and a very similar predicted secondary structure. The predicted DSUL structure is amazingly similar to that of ISG15 and it will be interesting to find out whether similar enzymes used for ISGylation/deISGylation, which are different from those required for sumoylation/desumoylation, are also involved in conjugation/deconjugation of DSUL. For example, ISG15 utilizes the E2 enzyme UBC8, whereas SUMO utilizes the single E2 enzyme UBC9 (Kim et al., 2004; Zhao, 2007). UBC7, as well as UBC9 which is likely to be involved in ZmSUMO1a/b conjugation, are expressed in the maize embryo sac (de Vries et al., 1998; Yang et al., 2006), but a gene encoding UBC8 has yet to be reported. Future work should thus aim to characterize the enzymatic DSUL maturation, activation, conjugation and deconjugation machinery. However, owing to the very specific and restricted expression pattern of *DSUL* in the FG, these efforts are biochemically limited and present a technical challenge.

Outlook

Loss- and gain-of-function studies in various organisms have resulted in an emerging paradigm that sumoylation regulates a number of developmental processes in both animals and plants (reviewed by Zhao, 2007; Miura et al., 2007). Although most biological processes regulated by sumoylation remain to be identified, T-DNA insertions in SUMO E2 enzymes or *sumo1/sumo2* double mutants, for example, cause early embryo lethality in *Arabidopsis* (Saracco et al., 2007). In animals, mutations of the single SUMO E2 enzyme UBC9 have been shown to lead to meiotic defects in the fruit fly as well as to embryonic lethality in *C. elegans* and mice (reviewed by Zhao, 2007). Moreover, in mammals, SUMO1 has been reported to be required for development of lip and palate during later embryonic stages (Alkuraya et al., 2006). Although a large number of reports are already available concerning diubiquitin-like ISG15 and FAT10, surprisingly little is known about their role in development. Mice homozygous for disruption of the *Fat10* gene are viable and fertile. Detailed studies revealed that lymphocytes were more prone to spontaneous apoptotic death and FAT10 was thus suggested to be a survival factor (Canaan et al., 2006).

Even less is known about sumoylation during gametogenesis. It has been shown that sumoylation is dynamic and likely to be involved in the modulation of gene expression during mammalian oocyte and spermatid growth and maturation, but functional data have not yet been provided (Ihara et al., 2008; La Salle et al., 2008). The role of sumoylation in plant male and female gametogenesis has not previously been investigated. Owing to the ubiquitous expression pattern of *ZmSUMO1a/b* and the expectation of obtaining numerous phenotypes and the lethality of *ZmSUMO1a/b*-RNAi silencing, we restricted our studies to *diSUMO-like* from maize, which is specifically expressed in the FG. Embryo sac development of *dsul* mutant ovules was terminated at stage FG 5/6, when the *ZmDSUL* promoter is activated. The plant hormone auxin has recently been shown to accumulate until this stage and to mediate FG patterning in *Arabidopsis*, with highest concentrations in the micropylar region (Pagnussat et al., 2009). We have studied the inducibility of the *ZmDSUL* promoter after auxin treatment (data not shown), but never observed marker gene expression, indicating that either components of the gene regulatory network are missing in suspension cells or that the promoter is not auxin inducible. Further experimentation is required to resolve this issue. Moreover, owing to the termination of mutant FG development at stage FG 5/6, it was not possible to study the role of ZmDSUL in mature eggs or during zygote development. The strongly increased expression pattern after fertilization indicates, however, that ZmDSUL is also likely to have post-zygotic functions that are probably correlated with asymmetric zygote division. A mature egg/zygote-specific loss-of-function approach will be required to address this question. Compared with the stages of megagametogesis, mature and fertilized egg cells are more easily accessible and might prove useful in identifying both DSUL targets and the corresponding enzymatic machinery.

Acknowledgements

We thank Stefanie Sprunck for helpful discussions and for providing wheat egg cell-expressed *DSUL* cDNA clones; Reinhold Brettschneider for seeds of a *pUbi:GUS* line; Svenja Rademacher for providing ER-GFP protein; Manfred Gahrtz and Kwang-Il Ri for generating the *pZmDSUL:GFP* construct and for maize transformation; Ulrich Hammes for critical comments on the manuscript; Matthew M. S. Evans for helpful suggestions for the histological studies; and Marco Bocola for the introduction to 3D protein modeling. This work was supported by a post-graduate scholarship to K.S. in accordance with Hamburg's Young Academics Funding Law and a CAPES fellowship to N.G.K.

Competing interests statement

The authors declare no competing financial interests.

Supplementary material

Supplementary material for this article is available at
http://dev.biologists.org/lookup/suppl/doi:10.1242/dev.035964/-/DC1

References

Alkuraya, F. S., Saadi, I., Lund, J. J., Turbe-Doan, A., Morton, C. C. and Maas, R. L. (2006). SUMO1 haploinsufficiency leads to cleft lip and palate. *Science* **313**, 1751.

Anckar, J. and Sistonen, L. (2007). SUMO: getting it on. *Biochem. Soc. Trans.* **35**, 1409-1413.

Bantin, J., Matzk, F. and Dresselhaus, T. (2001). *Tripsacum* as a natural model system to study parthenogenesis. *Sex. Plant Reprod.* **14**, 219-226.

Becker, D., Brettschneider, R. and Lörz, H. (1994). Fertile transgenic wheat from microprojectile bombardment of scutellar tissue. *Plant J.* **5**, 299-307.

Berger, F., Hamamura, Y., Ingouff, M. and Higashiyama, T. (2008). Double fertilization-caught in the act. *Trends Plant Sci.* **13**, 437-443.

Borges, F., Gomes, G., Gardner, R., Moreno, N., McCormick, S., Feijó, J. A. and Becker, J. D. (2008). Comparative transcriptomics of *Arabidopsis* sperm cells. *Plant Physiol.* **148**, 1168-1181.

Brettschneider, R., Becker, D. and Lörz, H. (1997). Efficient transformation of scutellar tissue of immature maize embryos. *Theor. Appl. Genet.* **94**, 737-748.

Brukhin, V., Curtis, M. D. and Grossniklaus, U. (2005). The angiosperm female gametophyte: no longer the hidden generation. *Curr. Sci.* **89**, 1844-1852.

Canaan, A., Yu, X., Booth, C. J., Lian, J., Lazar, I., Gamfi, S. L., Castille, K., Kohya, N., Nakayama, Y., Liu, Y. C. et al. (2006). FAT10/diubiquitin-like protein-deficient mice exhibit minimal phenotypic differences. *Mol. Cell. Biol.* **26**, 5180-5189.

Cordts, S., Bantin, J., Wittich, P. E., Kranz, E., Lörz, H. and Dresselhaus, T. (2001). *ZmES* genes encode peptides with structural homology to defensins and are specifically expressed in the female gametophyte of maize. *Plant J.* **25**, 103-114.

Desterro, J. M., Rodriguez, M. S., Kemp, G. D. and Hay, R. T. (1999). Identification of the enzyme required for activation of the small ubiquitin-like protein SUMO-1. *J. Biol. Chem.* **274**, 10618-10624.

de Vries, A., Cordts, S. and Dresselhaus, T. (1998). Molecular characterization of a cDNA encoding an ubiquitin carrier protein (UBC7) isolated from egg cells of maize (Accession No. AJ002959) (PGR98-177). *Plant Physiol.* **118**, 1011.

D'Halluin, K., Bonne, E., Bossut, M., De Beuckeleer, M. and Leemans, J. (1992). Transgenic maize plants by tissue electroporation. *Plant Cell* **4**, 1495-1505.

Dresselhaus, T., Lörz, H. and Kranz, E. (1994). Representative cDNA libraries from few plant cells. *Plant J.* **5**, 605-610.

Drews, G. N. and Yadegari, R. (2002). Development and function of the angiosperm female gametophyte. *Annu. Rev. Genet.* **36**, 99-124.

Evans, M. M. (2007). The *indeterminate gametophyte1* gene of maize encodes a LOB domain protein required for embryo Sac and leaf development. *Plant Cell* **19**, 46-62.

García-Mata, R., Bebok, Z., Sorscher, E. J. and Sztul, E. S. (1999). Characterization and dynamics of aggresome formation by a cytosolic GFP-chimera. *J. Cell Biol.* **146**, 1239-1254.

Geiss-Friedlander, R. and Melchior, F. (2007). Concepts in sumoylation: a decade on. *Nat. Rev. Mol. Cell Biol.* **8**, 947-956.

Gill, G. (2004). SUMO and ubiquitin in the nucleus: different functions, similar mechanisms? *Genes Dev.* **18**, 2046-2059.

Green, C. E. and Phillips, R. L. (1975). Plant regeneration from tissue cultures of maize. *Crop Sci.* **15**, 417-421.

Gross-Hardt, R., Kagi, C., Baumann, N., Moore, J. M., Baskar, R., Gagliano, W. B., Jurgens, G. and Grossniklaus, U. (2007). LACHESIS restricts gametic cell fate in the female gametophyte of *Arabidopsis*. *PLoS Biol.* **5**, e47.

Haglund, K. and Stenmark, H. (2006). Working out coupled monoubiquitination. *Nat. Cell Biol.* **8**, 1218-1219.

Hatakeyama, S. and Nakayama, K. I. (2003). Ubiquitylation as a quality control system for intracellular proteins. *J. Biochem.* **134**, 1-8.

Hay, R. T. (2005). SUMO: a history of modification. *Mol. Cell* **18**, 1-12.

Hendrickson, T. W., Yao, J., Bhadury, S., Corbett, A. H. and Joshi, H. C. (2001). Conditional mutations in gamma-tubulin reveal its involvement in chromosome segregation and cytokinesis. *Mol. Biol. Cell* **12**, 2469-2481.

Herrmann, J., Lerman, L. O. and Lerman, A. (2007). Ubiquitin and ubiquitin-like proteins in protein regulation. *Circ. Res.* **100**, 1276-1291.

Hipp, M. S., Kalveram, B., Raasi, S., Groettrup, M. and Schmidtke, G. (2005). FAT10, a ubiquitin-independent signal for proteasomal degradation. *Mol. Cell. Biol.* **25**, 3483-3491.

Holsters, M., Silva, B., Van Vliet, F., Genetello, C., De Block, M., Dhaese, P., Depicker, A., Inze, D., Engler, G., Villarroel, R. et al. (1980). The functional organization of the nopaline *A. tumefaciens* plasmid pTiC58. *Plasmid* **3**, 212-230.

Huang, B.-Q. and Sheridan, W. F. (1994). Female gametophyte development in maize: microtubular organization and embryo sac polarity. *Plant Cell* **6**, 845-861.

Hubbert, C., Guardiola, A., Shao, R., Kawaguchi, Y., Ito, A., Nixon, A., Yoshida, M., Wang, X. F. and Yao, T. P. (2002). HDAC6 is a microtubule-associated deacetylase. *Nature* **417**, 455-458.

Ihara, M., Stein, P. and Schultz, R. M. (2008). UBE2I (UBC9), a SUMO-conjugating enzyme, localizes to nuclear speckles and stimulates transcription in mouse oocytes. *Biol. Reprod.* **79**, 906-913.

Johnson, E. S. (2004). Protein modification by SUMO. *Annu. Rev. Biochem.* **73**, 355-382.

Johnston, J. A., Ward, C. L. and Kopito, R. R. (1998). Aggresomes: a cellular response to misfolded proteins. *J. Cell Biol.* **143**, 1883-1898.

Jones-Rhoades, M. W., Borevitz, J. O. and Preuss, D. (2007). Genome-wide expression profiling of the *Arabidopsis* female gametophyte identifies families of small, secreted proteins. *PLoS Genet.* **3**, 1848-1861.

Kalveram, B., Schmidtke, G. and Groettrup, M. (2008). The ubiquitin-like modifier FAT10 interacts with HDAC6 and localizes to aggresomes under proteasome inhibition. *J. Cell Sci.* **121**, 4079-4088.

Karimi, M., Inze, D. and Depicker, A. (2002). GATEWAY vectors for *Agrobacterium*-mediated plant transformation. *Trends Plant Sci.* **7**, 193-195.

Kawaguchi, Y., Kovacs, J. J., McLaurin, A., Vance, J. M., Ito, A. and Yao, T. P. (2003). The deacetylase HDAC6 regulates aggresome formation and cell viability in response to misfolded protein stress. *Cell* **115**, 727-738.

Kerscher, O. (2007). SUMO junction-what's your function? New insights through SUMO-interacting motifs. *EMBO Rep.* **8**, 550-555.

Kim, H. J., Oh, S. A., Brownfield, L., Hong, S. H., Ryu, H., Hwang, I., Twell, D. and Nam, H. G. (2008). Control of plant germline proliferation by SCF (FBL17) degradation of cell cycle inhibitors. *Nature* **455**, 1134-1137.

Kim, K. I., Giannakopoulos, N. V., Virgin, H. W. and Zhang, D. E. (2004). Interferon-inducible ubiquitin E2, Ubc8, is a conjugating enzyme for protein ISGylation. *Mol. Cell. Biol.* **24**, 9592-9600.

Kirkin, V. and Dikic, I. (2007). Role of ubiquitin- and Ubl-binding proteins in cell signaling. *Curr. Opin. Cell Biol.* **19**, 199-205.

Kranz, E., Bautor, J. and Lörz, H. (1991). In vitro fertilization of single, isolated gametes of maize mediated by electrofusion. *Sex. Plant Reprod.* **4**, 12-16.

La Salle, S., Sun, F., Zhang, X. D., Matunis, M. J. and Handel, M. A. (2008). Developmental control of sumoylation pathway proteins in mouse male germ cells. *Dev. Biol.* **321**, 227-237.

Leisner, C., Kammerer, D., Denoth, A., Britschi, M., Barral, Y. and Liakopoulos, D. (2008). Regulation of mitotic spindle asymmetry by SUMO and the spindle-assembly checkpoint in yeast. *Curr. Biol.* **18**, 1249-1255.

Liu, J., Zhang, Y., Qin, G., Tsuge, T., Sakaguchi, N., Luo, G., Sun, K., Shi, D., Aki, S., Zheng, N. et al. (2008). Targeted degradation of the cyclin-dependent kinase inhibitor ICK4/KRP6 by RING-type E3 ligases is essential for mitotic cell cycle progression during *Arabidopsis* gametogenesis. *Plant Cell* **20**, 1538-1554.

Márton, M. L., Cordts, S., Broadhvest, J. and Dresselhaus, T. (2005). Micropylar pollen tube guidance by egg apparatus 1 of maize. *Science* **307**, 573-576.

Matic, I., van Hagen, M., Schimmel, J., Macek, B., Ogg, S. C., Tatham, M. H., Hay, R. T., Lamond, A. I., Mann, M. and Vertegaal, A. C. (2008). In vivo identification of human small ubiquitin-like modifier polymerization sites by high accuracy mass spectrometry and an in vitro to in vivo strategy. *Mol. Cell. Proteomics* **7**, 132-144.

Melchior, F. (2000). SUMO-nonclassical ubiquitin. *Annu. Rev. Cell Dev. Biol.* **16**, 591-626.

Miura, K., Jin, J. B. and Hasegawa, P. M. (2007). Sumoylation, a post-transcriptional regulatory process in plants. *Curr. Opin. Plant Biol.* **10**, 495-502.

Müller, S., Hoege, C., Pyrowolakis, G. and Jentsch, S. (2001). SUMO, ubiquitin's mysterious cousin. *Nat. Rev. Mol. Cell Biol.* **2**, 202-210.

Murashige, T. and Skoog, F. (1962). A revised medium for rapid growth and bioassays with tobacco tissue cultures. *Physiol. Plant* **15**, 473-497.

Narasimhan, J., Wang, M., Fu, Z., Klein, J. M., Haas, A. L. and Kim, J. J. (2005). Crystal structure of the interferon-induced ubiquitin-like protein ISG15. *J. Biol. Chem.* **280**, 27356-27365.

Nicholas, K. B., Nicholas, H. B., Jr and Deerfield, D. W., II (1997). GeneDoc: analysis and visualization of genetic variation. *EMBNEW News* **4**, 14.

Page, R. D. (1996). TreeView: an application to display phylogenetic trees on personal computers. *Comput. Appl. Biosci.* **12**, 357-358.

Pagnussat, G. C., Yu, H. J., Ngo, Q. A., Rajani, S., Mayalagu, S., Johnson, C. S., Capron, A., Xie, L. F., Ye, D. and Sundaresan, V. (2005). Genetic and molecular identification of genes required for female gametophyte development and function in *Arabidopsis*. *Development* **132**, 603-614.

Pagnussat, G. C., Alandete-Saez, M., Bowman, J. L. and Sundaresan, V. (2009). Auxin-dependent patterning and gamete specification in the *Arabidopsis* female gametophyte. *Science* **324**, 1684-1689.

Pallotta, M. A., Graham, R. D., Langridge, P., Sparrow, D. H. B. and Barker, S. J. (2000). RFLP mapping of manganese efficiency in barley. *Theor. Appl. Genet.* **101**, 1100-1108.

Pastuglia, M., Azimzadeh, J., Goussot, M., Camilleri, C., Belcram, K., Evrard, J. L., Schmit, A. C., Guerche, P. and Bouchez, D. (2006). Gamma-tubulin is essential for microtubule organization and development in *Arabidopsis*. *Plant Cell* **18**, 1412-1425.

Saracco, S. A., Miller, M. J., Kurepa, J. and Vierstra, R. D. (2007). Genetic analysis of SUMOylation in *Arabidopsis*: conjugation of SUMO1 and SUMO2 to nuclear proteins is essential. *Plant Physiol.* **145**, 119-134.

Schwartz, D. C. and Hochstrasser, M. (2003). A superfamily of protein tags: ubiquitin, SUMO and related modifiers. *Trends Biochem. Sci.* **28**, 321-328.
Seeler, J. S. and Dejean, A. (2003). Nuclear and unclear functions of SUMO. *Nat. Rev. Mol. Cell Biol.* **4**, 690-699.
Sprunck, S., Baumann, U., Edwards, K., Langridge, P. and Dresselhaus, T. (2005). The transcript composition of egg cells changes significantly following fertilization in wheat (*Triticum aestivum* L.). *Plant J.* **41**, 660-672.
Tatham, M. H., Jaffray, E., Vaughan, O. A., Desterro, J. M., Botting, C. H., Naismith, J. H. and Hay, R. T. (2001). Polymeric chains of SUMO-2 and SUMO-3 are conjugated to protein substrates by SAE1/SAE2 and Ubc9. *J. Biol. Chem.* **276**, 35368-35374.
Thompson, J. D., Higgins, D. G. and Gibson, T. J. (1994). CLUSTAL W: improving the sensitivity of progressive multiple sequence alignment through sequence weighting, position-specific gap penalties and weight matrix choice. *Nucleic Acids Res.* **22**, 4673-4680.
Ulrich, H. D. (2008). The fast-growing business of SUMO chains. *Mol. Cell* **32**, 301-305.
Vertegaal, A. C., Andersen, J. S., Ogg, S. C., Hay, R. T., Mann, M. and Lamond, A. I. (2006). Distinct and overlapping sets of SUMO-1 and SUMO-2 target proteins revealed by quantitative proteomics. *Mol. Cell. Proteomics* **5**, 2298-2310.
Voinnet, O., Lederer, C. and Baulcombe, D. C. (2000). A viral movement protein prevents spread of the gene silencing signal in *Nicotiana benthamiana*. *Cell* **103**, 157-167.
Voinnet, O., Rivas, S., Mestre, P. and Baulcombe, D. (2003). An enhanced transient expression system in plants based on suppression of gene silencing by the p19 protein of tomato bushy stunt virus. *Plant J.* **33**, 949-956.
Vollbrecht, E. and Hake, S. (1995). Deficiency analysis of female gametogenesis in maize. *Dev. Genet.* **16**, 44-63.
Watts, F. Z. (2007). The role of SUMO in chromosome segregation. *Chromosoma* **116**, 15-20.
Welchman, R. L., Gordon, C. and Mayer, R. J. (2005). Ubiquitin and ubiquitin-like proteins as multifunctional signals. *Nat. Rev. Mol. Cell Biol.* **6**, 599-609.
Yang, H., Kaur, N., Kiriakopolos, S. and McCormick, S. (2006). EST generation and analyses towards identifying female gametophyte-specific genes in *Zea mays* L. *Planta* **224**, 1004-1014.
Young, B., Sherwood, R. T. and Bashaw, E. C. (1979). Cleared-pistil and thick-sectioning techniques for detecting aposporous apomixis in grasses. *Can. J. Bot.* **57**, 1668-1672.
Zeng, Y. X., Hu, C. Y., Lu, Y. G., Li, J. Q. and Liu, X. D. (2009). Abnormalities occurring during female gametophyte development result in the diversity of abnormal embryo sacs and leads to abnormal fertilization in indica/japonica hybrids in rice. *J. Integr. Plant Biol.* **51**, 3-12.
Zhang, F. P., Mikkonen, L., Toppari, J., Palvimo, J. J., Thesleff, I. and Janne, O. A. (2008). Sumo-1 function is dispensable in normal mouse development. *Mol. Cell. Biol.* **28**, 5381-5390.
Zhao, J. (2007). Sumoylation regulates diverse biological processes. *Cell Mol. Life Sci.* **64**, 3017-3033.